MODULATION OF UNSTRUCTURED PULSATIONS OF PC1 FREQUENCY RANGE BY IMF VARIATIONS: A CASE STUDY

© 2025 V. V. Safargaleev[a,b,] *

[a]*Pushkov Institute of Terrestrial Magnetism, Ionosphere and Radio Wave Propagation RAS, St. Petersburg Department, St. Petersburg, Russia*

[b]*Polar Geophysical Institute RAS, Apatity, Russia*

**e-mail: Vladimir.safargaleev@pgia.ru*

Received February 18, 2025

Revised May 07, 2025

Accepted May 22, 2025

Abstract. Structured pulsations in the frequence range 0–5 Hz such as "pearls" are of common occurrence and therefore well studied. On magnetograms, “pearls” look like a series of wave packets. Despite the numerous investigations, the question of the reasons for such modulation still remains. Less studied is another type of modulated *Pc*1, which appears on sonograms as a series of shapeless «clouds» without a pronounced internal structure (unstructured *Pc*1). At an early stage of research, unstructured *Pc*1 were considered primarily in the context of the response of the magnetosphere to the impact of a slow shock wave front on the magnetopause (SI event). It was subsequently shown that SI is not a necessary condition for the generation of this *Pc*1 subclass. In this work, unstructured modulated *Pc*1 observed both before and after SI were investigated. Using the favorable position of the GEOTAIL and THE satellites, it is shown that there are pressure variations with a repetition period of 12 minutes inside the magnetosphere, with which “clouds” of unstructured *Pc*1 are synchronized. There are no pressure variations on satellites in the solar wind. Instead, satellites record variations in IMF with the same period. Based on observations, a scenario for the phenomenon is proposed.

Keywords: *unstructured Pc1 pulsations, sudden pulses, solar wind, magnetospheric domains, equivalent ionospheric currents*

DOI: 10.31857/S00167940250508e5

1. INTRODUCTION

Short-period pulsations (*Ps1* pulsations) are electromagnetic waves with frequency in the range of 0.1-5 Hz. In contrast to long-period pulsations, which are most often standing waves, *Ps1*

pulsations are Alven waves propagating along the magnetic field (see, e.g., [Anderson et al., 1996]), which makes them potentially suitable for remote sensing of the magnetosphere from the Earth's surface (see, e.g., [Troitskaya and Gul'elmi, 1967]). This is the reason for the interest in the study of *Ps1*.

One of the features of Ps1 is amplitude modulation, manifested as a sequence of wave packets. Since in early analog recordings this form of activity resembled a pearl necklace, this type of *Ps1* was called "pearls" [Sucksdorff, 1936]. Studies using sonograms revealed the fine structure of each packet in the form of a series of short-term bursts of increasing (less often - decreasing) frequency. For this reason, the characteristic "structured" is still used for pearls (see, for example, [Kangas et al., 1998]). To date, a number of theories of pearl generation have been proposed (see [Guglielmi and Potapov, 2019] for a review). According to one theory, the periodic shape of pearls is due to modulation of the incremental ion-cyclotron instability of the magnetospheric plasma by *Pc4-band* waves [Lyatsky and Plyasova-Bakounina, 1986; Plyasova-Bakounina et al., 1996; Mursula et al., 2001] rather than to propagation of ion-cyclotron waves along the magnetic field force line with multiple reflections from conjugate ionospheres. The authors suggest that the modulating waves are the result of resonant amplification of a broadband signal penetrated into the magnetosphere from the interplanetary medium.

Less studied is another type of *Ps1* with amplitude modulation - unstructured pulsations, which have on sonograms the appearance of a series of formless spots (see, for example, Fig. 2 in [Safargaleev et al., 2002] and Fig. 1 in [Dovbnya and Zotov, 1985]), following one after another with an interval of 12-15 min. Following the proposed terminology [Fukunishi et al., 1981], this type of activity can be called as "bursts of hydromagnetic emissions". In [Dovbnya & Zotov, 1985], it was proposed to call this subclass of Hertz oscillations as *Pc1S* pulsations, where the prefix *S* stands for *spot*. In [Safargaleev et al., 2002], the term "*Psi1* pulsations" was used, emphasizing their connection with SI (*sudden impulse*) events. Hereafter, we will use the term "spots" or *Pc1S*. Often these pulsations are observed as a response of the magnetosphere to a solar wind pressure spike (see, for example, [Parkhomov et al. 2010]), indicating that their trigger should be sought in the interplanetary medium. The period of succession of the spots noticeably exceeds the range of *Pc5* pulsations, which in this geophysical context represent the resonance oscillations of the magnetosphere.

The currently accepted cause of *Pc1* generation during SI is considered to be the development of ion-cyclotron plasma instability as a result of the "compression" of the magnetic force tube [Olson and Lee, 1983] in the magnetosphere contracting under the influence of the solar wind. Therefore, based on the results of [Plyasova-Bakounina et al., 1996], it is logical to try to find signs of a modulating wave, first of all, in variations of the solar wind pressure. In [Safargaleev

et al., 2002], such an attempt was not successful− signs of a modulating wave could not be detected either in the solar wind or in the data of magnetometers located in the region of registration of *Pc1* spots (subauroral zone). Further studies have shown that *Pc1S* can appear irrespective of the solar wind pressure spike. For example, in [Safargaleev & Tereshchenko, 2019] it is shown that *Pc1S* appeared after about an hour c of SI (see Fig. 4 in the cited paper). Below we study the case when *Pc1S* spots are visible on sonograms both before and after the SI moment. The pressure jump may not be accompanied by the generation of spots at all (see, for example, Fig. *1a* in [Safargaleev et al., 2003]). All this indicates that a sudden increase in solar wind pressure is not a necessary condition for triggering the *Ps1S* series. In this connection, we note the work [Safargaleev & Tereshchenko, 2019], where the variation of the Bz *component of* the interplanetary magnetic field on the THEMIS (*Time History of Events and Macroscale Interactions during Substorms*) satellite was suggested to be a sign of a modulating wave.

The objectives of the work are as follows. Using the successful mutual position of the GEOTAIL and THEMIS E satellites (hereafter referred to as THE), to show the presence of wave activity in the magnetosphere in the form of pressure variations, while in the solar wind the variations of plasma parameters are not identified, but the variations of the interplanetary magnetic field (IMF) with approximately the same period are detected. Demonstrate the relationship of pressure variations with the modulation of unstructured Ps1, as well as with variations in the *X-component* in the high-latitude part of the IMAGE magnetometer network. Using *Defense Meteorological Satellite Program* (DMSP) satellite data, determine with which intramagnetospheric structure the high-latitude long-period pulsations are most likely associated.

2. DATA AND METHODOLOGY

The main instrument of the study is the induction magnetometers of the Polar Geophysical Institute of the Russian Academy of Sciences installed on the Kola Peninsula (obs. Lovozero, LOZ, geographic coordinates 67.97° N, 35.08° E) and on the Svalbard Archipelago (obs. Barentsburg, BAB, geographic coordinates 78.09° N, 14.21° E). The magnetometers continuously record the geomagnetic field variations with temporal discretization of the signal at 40 samples per second. The data were used to present the *Pc1* range pulsations in the form of sonograms (dynamic spectra).

Long-period pulsations were investigated using data from the IMAGE network magnetometers (https://space.fmi.fi/MIRACLE). The coordinates of the stations can be found on the corresponding page of this site. At the same site, the distribution of ionospheric equivalent currents was plotted in the online mode.

During the event, the solar wind inhomogeneity front hit the magnetopause, at which the solar wind pressure increases rapidly (*sudden impulse*, SI). To confirm the fact of the interaction of the inhomogeneity front with the magnetosphere, data from the low-latitude station Addis Ababa (AAE, 09.04° N, 38.77° E) were used. We do not specify the type of inhomogeneity here, since it is not fundamental for the issue under consideration - the search for a modulating wave, including half an hour before the moment of impact. For example, according to [Parkhomov et al. 2018; 2021], such inhomogeneity can be an interplanetary shock wave or a diamagnetic structure, respectively.

The choice of this particular interval among others is due to the fortunate position of the GEOTAIL and THE satellites, which is a rare event (see comments in [Eastwood et al., 2008]. The positions of the satellites relative to each other, the magnetopause, and the shock front were determined using the online procedure *SSC 4D Orbit Viewer* (https://sscweb.gsfc.nasa.gov). The position of the satellites is presented in Fig. 1 for two moments of time - before and after SI. Data from the WIND satellite, which is located at a significant distance from the magnetopause, were also used.

Fig. 1.

The DMSP series satellites fly in near-polar orbits at an altitude of 840 km and record the ejected particles in the energy range from 30 eV to 30 keV with a *temporal* resolution of 1 s. An automatic algorithm proposed in [Newell et al., 1991] was used to determine the boundaries of auroral intrusions (magnetospheric domains). The algorithm was tested for pre-midday rashes [de la Beaujardiere et al., 1993]. Note also that, according to statistical studies (see Fig. 2 in [Newell and Meng, 1992]), in the 9-12 MLT interval, the boundaries of magnetospheric domains are oriented predominantly along the geomagnetic latitude. The phenomenon analyzed in this work took place in this MLT interval.

The DMSP data in the form of spectrograms indicating the domain boundaries were obtained from the site of J. Hopkins University (http://sd-www.jhuapl.edu/Aurora/spectrogram/index.html). The spectrograms show the coordinates of the subsatellite point, from which the projection of the satellite along the force line to the height of the *E-layer* of the ionosphere was calculated at a known satellite height. For such heights, it is sufficient to use only the IGRF model of the force line in the projection.

We will assume that a periodic perturbation of the pressure or magnetic field on the satellite and/or on the Earth's surface is a sign of a modulating wave if the period of the perturbation is close to the period of succession of *Ps1* spots, and they begin simultaneously. In other words, if the *Pc1S* pulsations and the field and/or pressure variations show synchrony.

3. MEASUREMENT RESULTS

3.1 Unstructured Pc1 pulsations. Signs of a modulating wave in the ground magnetic data

The shape and dynamics of unstructured *Ps1* in the WAV and LOZ are presented in the sonograms in Fig. *2a*. Relying on the results of [Safargaleev et al., 2010] and [Parkhomov et al., 2018], the SI moment (T_{SI}~ 07:04:00 UT) was defined as the beginning of the burst in the 0-0.35 Hz range in the LOZ and the beginning of the negative SI pre-pulse in the NAL magnetogram. This moment is indicated in Fig. *2a* by the vertical line. After about one minute, the induction magnetometers register a brief burst in the 0-4 Hz range, marked on the LOZ sonogram by the white numeral 1, and a rapid increase of the *X-component of* the magnetic field begins at the AAE station. This sequence of perturbations is typical for SI [Safargaleev et al., 2010].

The dynamics of Pc1 pulsations before and after SI is different. Further we will consider these two hourly intervals separately. Before $T_{SI}$the general picture of *Ps1* is rather simple. The sonograms show several series of unstructured Pc1 spots at different carrier frequencies (~1 Hz, 1.2 Hz, 1.8 Hz, and 3 Hz). The frequency bandwidth of *Pc1S* Δ f ~ 0.3-0.5 Hz, with a period of ~12 min. We do not emphasize the fact that *Pc1S* are presented differently on different sonograms. For example, a series at the carrier frequency of 2 Hz is not visible or not as pronounced in the WAV. The series of two spots at 3 Hz in the WAB is not visible in the LOZ. The most important point, which we consider a sign of a modulating wave, is the synchronous appearance of *Pc1S* at different frequencies, and approximately the same period of succession.

After SI, the shape of the activity becomes more complex. The LOZ sonogram shows a series of three bursts at a carrier frequency of ~1 Hz. The series looks like a continuation of the series at this frequency before SI, but differs from it by a longer period of succession (~17 min). In addition, this series is "swept" by another series, which we leave without attention. On the sonogram, the bursts are marked with white figures 2, 3, and 4. This frequency range is hidden by noise on the BAB sonogram. Synchronously with bursts 3 and 4, a series of two bursts at the carrier frequencies of 2.1 and 3 Hz can be distinguished at both stations. These bursts are labeled with the same numbers as the bursts in the "low frequency" series. The series at 3 Hz looks like a continuation of the series at the same frequency until SI. Here we also emphasize the simultaneity of bursts 3 and 4 in all three series and the roughly similar period of succession.

If we assume that the observed amplitude modulation of *Pc1* is the result of the influence of a modulating wave on the magnetospheric plasma, then the different period of succession of the spots in the *Pc1S* event before and after SI may indicate that different modulating waves took part in their generation.

We consider the variations of the *X-component* at high and low latitudes (bottom two panels in Fig. *2a*) to be another sign of a modulating wave in terrestrial magnetic data. The magnetogram

of only the highest-latitude station (NAL) is shown here as an example. The magnetograms of other stations in the IMAGE network, as well as the dynamics of ionospheric equivalent currents corresponding to magnetic perturbations, will be discussed in Section *3.3.*

Up to the SI moment, the variations in the NAL practically coincide with the series of *Pc1S* spots on the LOZ and BAB sonograms. This picture resembles the situation from [Plyasova-Bakounina et al., 1996], where Fig. 7 demonstrates the relationship of "pearls" with *Pc4* pulsations. There is no variation in AAE before SI (lower panel in Fig. *2a*). After SI, it is not possible to correlate *Pc1S* in LOZ and UAE with any variations in NAL. On the contrary, the observation intervals of *Pc1S* spots 3 and 4 in LOZ and UAE can be compared with two weak, but detectable to the naked eye, variations in AAE some time after SI (highlighted in gray on the AAE magnetogram).

Fig. 2.

3.2 Signs of a modulating wave in the magnetosphere and in the solar wind

The first result of the study of this question (and of the work as a whole) is the detection of variations (waves) of the plasma pressure on THE satellite located inside the magnetosphere in the vicinity of the magnetopause (Fig. 1, upper panel). The variations are clearly visible in the first half of the interval (Fig. *2b*, upper panel). Their good correlation, close to coincidence when the plots are combined (Fig. *3a*), indicates that the shape of the ground disturbances in the LOZ, BAB, and NAL in Fig. *2a* is due to variations in the magnetospheric pressure. In Fig. *3a* we present the HOR magnetogram, where the amplitude of the long-period pulsations is maximum.

Fig. 3.

Note that we judge THE's position relative to the magnetopause not only from the results of calculations using the *SSC 4D Orbit Viewer* program (Fig. 1), but also from the rapid decrease in pressure on the satellite (Fig. *2b*, upper panel), which we interpret as the satellite's exit into the transition region as a result of the magnetopause's displacement toward the Earth. In addition, we associate the change of the sign of the Bz *component* on THE from positive (inside the magnetosphere) to negative (Fig. 4, bottom panel) with the crossing of the magnetopause, which could be due to the DCF current on the magnetopause surface. The sign change occurred at T_{MP}~ 07:04:24 UT, when THE (and thus the magnetopause) was at a distance ofΔ X~*19*.7 $R_E$from GEOTAIL. At a solar wind speed of 520 km/s (see Fig. *2b*), we obtain the propagation time of the perturbation from GEOTAIL to the magnetopause $\Delta T \sim 240$ c. This estimate will be needed later in a more accurate comparison of the interplanetary medium parameter variations at GEOTAIL with ELF activity in the form of *Pc1S* in the second half of the studied interval.

Fig. 4.

The second result– is the absence of corresponding pressure variations in the solar wind. The conclusion is based on the analysis of data from the GEOTAIL (two lower panels in Fig. *2b*) and WIND (Fig. *2c*, lower panel) satellites. Note that the plots are constructed without taking into account the time of propagation of perturbations from the satellites to the magnetopause. When comparing satellite data with ground-based data in the first half of the studied interval, one can easily orient oneself by SI, clearly visible in both Geotail and WIND data.

In the absence of pressure variations in the solar wind, terrestrial perturbations (*Ps1S* and long-period pulsations), as well as magnetospheric pressure variations on THE, correlate well with the variations of the MMP components on the satellites in the solar wind Fig. *2b* (middle three panels) and Fig. *2c* (top three panels). This is the third result. Note that the variation of the Bz *component of the* MMP has the smallest amplitude both near the magnetopause and at a significant distance from it. Traditionally, the Bz-component is considered to be the most geoeffective component of the IMF.

The second half of the interval (after SI) is characterized by a more complicated for analysis picture of magnetic perturbations both in the Hertz range and in the range of long-period pulsations. In contrast to the first half of the interval, *Ps1S* is more correlated directly with solar wind pressure variations on both GEOTAIL and WIND. In this case, spots 3 and 4 in Fig. *2a* can be regarded as the result of multiple magnetospheric compression. The above is demonstrated in Fig. *3*б. The variations in the *X component* at station AAE, highlighted in gray in the lower panel of Fig. *2a*, support this assumption.

On the satellites, one can also identify MMP variations similar to those that took place before the SI. The variations in the Bx *component* on GEOTAIL have a more distinct appearance and maximum amplitude. Note that the GEOTAIL data are given taking into account the time of perturbation propagation from the satellite to the magnetopause. The variations of № 2, 3 in Fig. *3b* can be compared with spots with the same numbers in the LOZ sonogram (Fig. *2a*). Whether the variations of the *Bx* component *of the* MMP on GEOTAIL were accompanied by variations of the pressure inside the magnetosphere, we cannot say, since THE satellite was already in the transition region.

Thus, the modulation of the unstructured *Ps1S* before SI can be attributed to MMP variations, and after SI we can consider the modulation as a result of the joint action of the three-stage compression of the magnetosphere by the solar wind and MMP variations.

3.3 The position of the source of 12 minute pulsations in the magnetosphere

To determine the approximate position of the source of long-period pulsations in the first half of the interval (up to the SI moment), we used the picture of the distribution of equivalent

ionospheric currents (ECLAT project) and the projection of the rush boundaries (DMSP F17). Hereafter, for brevity, we will omit the characterization "equivalent", each time referring to it.

The shape of the pulsations at the meridional chain of IMAGE stations and the diagram characterizing the position and dynamics of ionospheric currents corresponding to the pulsations are presented in Fig. 5. The magnetograms are arranged as the station latitude decreases so that the magnetogram of the highest-latitude station NAL is given in the upper part of the figure. Station coordinates can be taken from the IMAGE project website if necessary; the position of the NAL-MUO stations is shown on the map in Fig. *6*б. The white lines in the diagram are the geographic latitude of the station whose code is shown on the right. Figures in color here and below are available in the electronic version of the paper.

Fig. 5.

The diagram shows the presence of two types of pulsations, which is difficult to see by analyzing only the magnetograms in Fig. *5*a. Throughout the entire interval, the diagram shows pulsations with a period of 350-400 c, which correspond to the eastward current having a maximum approximately at latitude BJN. We believe that these pulsations are not relevant to the issue under consideration. The ripples with a period of ~750 c, which we regard as a sign of a modulating wave, begin at ~06:25 UT. The current corresponding to the ripples also flows in an easterly direction, but has a maximum at higher latitudes, somewhere between HOP and HOR.

Pulsations with approximately the same period can be identified in the magnetograms of NOR and at stations located to the south (Fig. *5a*). Here they occur in counter-phase relative to the stations poleward of the BJN, have an amplitude 5 times smaller (~30 nTL in NOR vs. ~150 nTL in HOR) and are therefore practically indistinguishable in the diagram. Only the NOR station is labeled on the diagram. At stations south of NOR, the amplitude of the pulsations is even smaller. The absence of measurements between BJN and NOR does not allow us to definitely answer the question where the change of sign of the ionospheric current associated with the 12-min pulsations occurs. A longitudinal current could flow at this boundary, which would clarify the nature of these pulsations.

Based on the available data, it can be argued that the 12-min pulsations on the IMAGE network are not associated with an Alven wave bouncing between conjugate ionospheres, since the period of such a wave would have to depend markedly on latitude. In the case under consideration, the period of pulsations at the lowest-latitude TAR station is the same as at the highest-latitude NAL station and is ~750 c both there and there. Note that the period of the spots in the LOZ sonogram is the same as in the BAB (Fig. *2a*, upper panel), which agrees with the result obtained in [Dovbnya & Zotov, 1985] regarding the independence of the latitude period of the *Pc1S* pulsations.

Fig. 6.

During a series of 12-minute pulsations, the DMSP F17 satellite flew over the Scandinavian Peninsula. This moment is marked in Fig. *5a* with an arrow, the width of which approximately corresponds to the time of the flyby over the observation area. The corresponding time interval is indicated in the spectrogram in Fig. *6a* and in the caption of Fig. *6*б. The spectrogram shows that at first the satellite was in a region of rushes characteristic of the *boundary plasma sheet* (bps). At about 06:50:10 UT, remaining inside the bps, the satellite flew into the region of energetic (>10 keV) ions. This moment is marked on the spectrogram by a vertical line with the number 1 in a circle. The projection of the satellite at the moment of flight into the region of ion spallings is shown on the distribution of ionospheric currents in Fig. *5b* with a black asterisk. In Fig. *6b* shows the position of magnetic stations relative to this boundary, also indicated by the number 1 in a circle. The solid line is the geomagnetic latitude of the point of intersection of the precipitation boundary. In this MLT sector, the geomagnetic latitude is oriented approximately along the boundaries of the magnetospheric domains [Newell and Meng, 1992]. Comparing Fig. 5 and Fig. 6, we can conclude that the region of pulsations with periods of ~750 s is projected in bps and is separated from the region of pulsations with period ~ 350-400 c by the poleward boundary of ionic precipitations. According to the F17 data, the change of sign of the 12-min pulsations could occur both at the bps/cps boundary and at the equatorial boundary of energetic (>1000 eV electrons) precipitations, labeled in Fig. 6 with the number 2.

The trajectory of F17 does not allow us to determine in which magnetospheric domain THE satellite was located at the time of registration of pressure variations. Having no identical induction magnetometers between the mainland and Svalbard, we also cannot determine the location of the ionospheric projection of the source of the studied *Ps1*. Therefore, we assume that it was located where the long-period pulsations had a maximum, i.e., in the vicinity of HOR and HOP. At higher (BAB) and lower latitudes (LOZ), the corresponding signal arrived via the ionospheric waveguide or, under certain conditions, via the near-equatorial waveguide formed under the plasmospheric vault [Guglielmi and Potapov, 2012]. The latitude of the BAB is approximately the same as that of the LYR of Fig. *5b*, and LOZ is located south of NOR, at approximately the same latitude as the MUO of Fig. *5a*.

4. DISCUSSION

4.1 Pc1S generation scenarios

One of the main parameters that determine Hertz wave generation is the transverse anisotropy of the particle temperature. An increase in anisotropy is often observed during solar wind pressure increases (SI events), when the daytime magnetosphere is compressed and the

magnetic field increases within the magnetosphere near the equatorial plane [Olson and Lee, 1983]. The increase of the magnetic field is manifested on the magnetograms of low-latitude stations as a rapid amplification of the X component. On sonograms of induction magnetometers, the response to SI has the form of a short-term single broadband burst [Tepley and Wentworth, 1962].

Several fortunate circumstances accompany the event under investigation.

First, the unstructured modulated *Ps1* occurred both before and after the magnetospheric compression by the rapid increase in solar wind pressure.

Second, the GEOTAIL and THE satellites were in a fortunate position. The former made measurements in the solar wind at a relatively small distance from the shock front, while the latter was inside the magnetosphere in the vicinity of the magnetopause and flew into the transition region after the SI.

Third, shortly before SI, the DMSP satellite flew over the observation area, crossing the rash boundaries.

The interval can be conditionally divided into two parts - before SI and after SI. The question about the cause of *Pc1* modulation after SI is more straightforward. Indeed, in Fig. *2a* and Fig. *3b* the spots of unstructured Ps1 Nos. 1, 3, and 4 are synchronized with the positive concentration pulses on the GEOTAIL satellite. It can also be argued that spots #1, #3, and #4 are related to solar wind pressure variations on the WIND satellite (Fig. *2c*). Such a connection has long been known and is explained directly by the compression of the magnetosphere by solar wind pressure pulses. The spot№ 2 is observed against a background of unchanging solar wind plasma concentration.

To understand the reason for the appearance of the № 2 spot, let us turn to the first half of the interval (up to SI), where *Pc1S* also occur against the background of unperturbed solar wind. At this time, THE satellite was inside the magnetosphere, and the pressure variations, synchronous with which the spots *P c* 1 appear, were registered on it. These variations are synchronized with the MMP variations on GEOTAIL and WIND.

Thus, the modulating perturbation for unstructured *Pc1* both before and after SI are periodic perturbations of the magnetospheric plasma pressure. In the second half of the interval, they are caused directly by solar wind pressure variations (multiple magnetospheric compression). We believe that in the first half of the interval, the pressure variations are initiated by the MMP variations.

The results of numerical simulations [Lin et al., 1996] showed that even if pressure variations are absent in the solar wind, they can be initiated by MMP variations in the transition region. Note also the work [Eastwood et al., 2008], where the phenomenon of *hot flow anomalies*,

HFA, is considered as a possible cause of the appearance of pressure variations in the transition region in the absence of such variations in the solar wind. Only one case is described in detail in the paper. The authors justify such a small statistic by the fact that the situations when the satellites are successfully located: one in the solar wind, the other in the transition region, are rare.

The appearance of pressure variations can also be given a simple physical explanation. Near the magnetopause there is a region of enhanced magnetic field - a magnetic barrier. To maintain a balance of total pressure inside and outside the magnetosphere, the plasma density and the magnitude of the field in the magnetic barrier must be related, and a change in the field will cause a change in pressure.

4.2 Note on the magnetic barrier

In Fig. 4, the interval including the moment when THE crossed the magnetopause is presented with a higher temporal resolution, which allows us to consider an interesting detail in the behavior of the *Bz* and *By* components. At the moment 07:05:29 UT, i.e., about a minute after crossing the magnetopause, the satellite registers a short-term deviation of *Bz* and *By by* $\Delta Bz \sim \Delta By \sim +5$ nTL. We attribute this short-term positive pulse in *Bz* and *By* (marked in gray in Fig. 4) to the satellite crossing the magnetic barrier. If we assume that the magnetic barrier was a product of the solar wind flowing around the magnetosphere and not the result of its sudden compression (i.e., it existed before the SI), then the above qualitative hypothesis about the role of the magnetic barrier in transforming the MMP variations into pressure variations inside the magnetosphere has the right to exist.

4.3 Remark on the multiplet character of Ps1S

As can be seen from Fig. *2a*, the phenomenon under study has a multiplet character. There are two traditional mechanisms explaining the generation of multiplet "pearls": ionospheric waveguide propagation of *Pc1* waves from several sources located in the equatorial magnetosphere [Greifinger and Greifinger, 1968; Ermakova et al., 2019] and spectral splitting by heavy magnetospheric ions He^+ and O^+ [Young et al., 1981]. In contrast to the "pearls", the unstructured Pc1S occupy a wider frequency band and from this position resemble the so-called spectral resonance structures, whose generation is attributed to the excitation of the ionospheric Alwen resonator. Note that multiplet "pearls" are also explained by the ionospheric Alvenov resonator (see, for example, [Prikner et al., 2004]). Under certain conditions, Hertz-range waves of complex structure can arise in an ion-cyclotron resonator with a discrete oscillation spectrum, which arises high above the Earth, in the equatorial part of the magnetosphere [Guglielmi and Potapov, 2012].

We believe that the multiplicity is determined by the peculiarities of the magnetospheric plasma - the existence of several sources in the magnetosphere, the presence of impurities, and the state of the ionosphere - rather than by the peculiarities of the modulating wave, which is the object of our study. Therefore, we leave the important and as yet unexplored question of the multiplet character of unstructured *Ps1S* out of the scope of our study, limiting ourselves to the brief comment made above.

5. CONCLUSION

Let us list the main results of the work.

1. We have analyzed jointly with satellite observations the pulsations of the Hertz range of *Pc1S*, which have on sonograms the form of a series of bursts (spots) with a period of succession lying outside the range of *Pc5* pulsations. The bursts do not have a pronounced internal structure. In the literature, such pulsations were studied in the context of magnetic storms or sudden compressions of the magnetosphere (SI) and were not systematic, being mainly case studies. In our case, *Pc1S* pulsations were observed both during and after SI, indicating that a solar wind pressure spike is not a necessary condition for their generation. In addition, their appearance was not associated with a magnetic storm. The study is aimed at finding the causes of the modulation and also has the status of a case study.

2. It is shown that the modulation of unstructured *Ps1* after SI could be caused directly by solar wind pressure variations ("multiple compressions" of the magnetosphere according to the terminology of [Yakhnin et al., 2019]). The result is not new.

3. Solar wind pressure variations were not observed before SI. Instead, variations of the MMP were observed. Synchronously with them, pressure variations from THE satellite data, long-period pulsations with maximum amplitude at the high-latitude part of the IMAGE network, and a series of unstructured *Ps1* spots on the Kola Peninsula and on Spitsbergen Island were observed inside the magnetosphere.

4. Determination of the position of the *Ps1S* source in the magnetosphere is not the goal of the work. The absence of identical induction magnetometers between the mainland and the northern tip of Svalbard does not allow us to do this more or less definitely. The analysis of the DMSP satellite ejections showed that the maximum of long-period pulsations is located in the plasma boundary layer (bps) to the pole from the energetic ion ejection boundary, i.e., in the vicinity of HOR and HOP in the projection to the ionosphere. Note that such a high-latitude position of the maximum of long-period pulsations explains the failure of the search for terrestrial signs of the modulating wave in [Safargaleev et al., 2002], which was conducted in the subauroral zone.

Considering these pulsations as a sign of the modulating wave, we assume that the source of *Pc1S* is located there, and in the BAB and LOZ the *Pc1* wave came through the ionospheric waveguide.
5. The study adds to the so far small statistics on the experimental confirmation of the theoretical hypothesis of the transformation in the transition region of MMP variations into pressure variations ([Eastwood et al., 2008]).

ACKNOWLEDGEMENTS

The author thanks P.T. Newell (Johns Hopkins University, APL, Laurel, Maryland, US) for preparing and posting on the Internet the information on the position of auroral eruption boundaries from DMSP satellite observations. THEMIS E, GEOTAIL and WIND data were taken from the world database CDAWeb (providers V. Angelopoulos, K. Ogilvie, NASA; A. Koval, UMBC; L. Frank, U. Iova). IMAGE data are available online (https://space.fmi.fi/MIRACLE). AAE station data were taken from the INTERMAGNET world database. Satellite positions were determined using the *SSC 4D Orbit Viewer* online procedure (https://sscweb.gsfc.nasa.gov). The author thanks Yu. V. Fedorenko (PGI) for help in preparing the data from the LOZ and BAB magnetometers.

FUNDING

The work was performed within the framework of the State Assignment (№ 1021100714196-5).

REFERENCES

1. *Guglielmi A.V., Potapov A.S.* The influence of heavy ions on the spectrum of magnetospheric vibrations // Space Research. V. 50. No. 4. P. 283-291. 2012. https://doi.org/10.1134/S0010952512040016

2. *Guglielmi A.V., Potapov A.S.* Problems of the theory of magnetospheric waves Rs1. Review // Solar-terrestrial physics. V. 5. No. 3. P. 102-109. 2019. https://doi.org/10.12737/szf-53201910

3. *Dovbnya B.V., Zotov O.A.* On a new type of geomagnetic pulsation Rs1 // Geomagnetism and aeronomy. V. 25. No. 3. P. 440-444. 1985.

4. *Ermakova E.N., Demekhov A.G., Yakhnina T.A., Yakhnin A.G., Kotik D.S., Raita T.* Features of dynamics of Pc1 multiband pulsation spectra in the presence of multiple ion-cyclotron instability regions in the magnetosphere // Izvestiya vysshikh uchebnykh zavedeniy. Radiophysics. V. 62. No. 1. P. 1-28. 2019.

5. *Lyatsky V.B., Plyasova-Bakunina T.A.* Influence of Pc4 magnetic pulsations on Pc1 generation // Geomagnetism and aeronomy. V. 26. No. 5. P. 802–804. 1986.

6. *Parkhomov V.A., Zastenker G.N., Ryazantseva M.O., Tsegmed B., Popova T.A.* Bursts of geomagnetic pulsations in the frequency range 0.2–5 Hz associated with large surges in solar

wind pressure // Space Research. V. 48. No. 1. P. 86-100. 2010. https://doi.org/10.1134/S0010952510010077

7. *Parkhomov V.A., Borodkova N.L., Yakhnin A.G., Raita T., Tsegmed B., Khomutov S.Yu., Pashinin A.Yu., Chilikin V.E., Mochalov A.A.* Two types of response of the magnetosphere in geomagnetic pulsations PSc to interaction with interplanetary shock waves // Solar-terrestrial Physics. V. 4. No. 3. P. 68-83. 2018. https://doi.org/10.12737/szf-43201808

8. *Parkhomov V.A., Yeselevich V.G., Yeselevich M.V., Dmitriev A.V., Suvorova A.V., Khomutov S.Yu., Tsegmed B., Raita T.* Magnetospheric response to interaction with the diamagnetic structure of the sporadic solar wind // Solar-terrestrial Physics. 2021. V. 7. No. 3. P. 12-30. 2021. https://doi.org/10.12737/szf-73202102

9. *Safargaleev V.V., Vasiliev A.N., Pchelkina E.V., Serebryanskaya A.V.* Geomagnetic pulsations of the 0.1–5 Hz range induced by a pulse of dynamic pressure of the solar wind // Geomagnetism and aeronomy. V. 43. No. 4. P. 482-492. 2003.

10. *Safargaleev V.V., Tereshchenko P.E.* Pulsations of the Hertzian range on the recovery phase of the magnetic storm 7-8.09.2017 and the relationship of their dynamics with changes in the parameters of the interplanetary medium // Geomagnetism and Aeronomy. V. 59. № 3. P. 301-315. 2019. https://doi.org/10.1134/S001679401903012X

11. *Yakhnin A.G., Titova E.E., Demekhov A.G., Yakhnina T.A., Popova T.A., Lyubchich A.A., Manninen Yu., Raita T.* Simultaneous observations of EMITS and VLF/UHF waves and eruptions of energetic particles during multiple compressions of the magnetosphere // Geomagnetism and Aeronomy. V. 59. No. 6. P. 714-726. 2019. https://doi.org/10.1134/S0016794019060142

12. *Anderson B., Denton R., Ho G., Hamilton D., Fuselier S., Strangeway R.* Observational test of local proton cyclotron instability in the Earth's magnetosphere // J. Geophys. Res. – Space. V. 101. № 10. P. 21527–21543. 1996. https://doi.org/10.1029/96JA01251

13. *de la Beaujardiere O., Watermann J., Newell P., Rich F.* Relationship between Birkeland current regions, particle precipitation, and electric field // J. Geophys. Res. – Space. V. 98. № 5. P. 7711–7720. 1993. https://doi.org/10.1029/92JA02005

14. *Eastwood J.P., Sibeck D.G., Angelopoulos V. et al*. THEMIS observations of a hot flow anomaly: Solar wind, magnetosheath, and ground-based measurements // Geophys. Res. Lett. V. 35. № 17. ID L17S03. 2008. https://doi.org/10.1029/2008GL033475

15. *Fukunishi H., Toya T., Koike K., Kuwashima M., Kawamura M.* Classification of hydromagnetic emission based on frequency-time spectra // J. Geophys. Res. – Space. V. 86. № 11. P. 9029–9039. 1981. https://doi.org/10.1029/JA086iA11p09029

16. *Greifinger C., Greifinger P.* Theory of hydromagnetic propagation in the ionospheric waveguide // J. Geophys. Res. V. 73. № 23. P. 7473–7490. 1968. https://doi.org/10.1029/JA073i023p07473

17. *Kangas J., Guglielmi A. Pokhotelov O.* Morphology and physics of short-period magnetic pulsations // *Space Sci. Rev.* V. 83. № 3–4. P. 435–512. 1998. https://doi.org/10.1023/A:1005063911643

18. *Lin Y., Swift D.W., Lee L.C.* Simulation of pressure pulses in the bow shock and magnetosheath driven by variations in interplanetary magnetic field direction // J. Geophys. Res. – Space. V. 101. № 12. P. 2725–27269. 1996. https://doi.org/10.1029/96JA02733

19. *Mursula K., Bräysy T., Niskala K., Russell C.T.* Pc1 pearls revisited: Structured electromagnetic ion cyclotron waves on Polar satellite and on ground // J. Geophys. Res. – Space. V. 106. № 12. P. 29543–29554. 2001. https://doi.org/10.1029/2000JA003044

20. *Newell P.T., Wing S., Meng C.-I., Sigilitto V.* The auroral oval position, structure and intensity of precipitation from 1984 onward: an automated on-line base // J. Geophys. Res. – Space. V. 96. № 4. P. 5877–5882. 1991. https://doi.org/10.1029/90JA02450

21. *Newell P.T., Meng C.-I.* Mapping the dayside ionosphere to the magnetosphere according to particle precipitation characteristics // Geophys. Res. Lett. V. 19. № 6. P. 609–612. 1992. https://doi.org/10.1029/92GL00404

22. *Olson J., Lee L.* Pc1 wave generation by sudden impulses // Planet Space Sci. V. 31. № 3. P. 295–302. 1983. https://doi.org/10.1016/0032-0633(83)90079-X

23. *Plyasova-Bakounina T.A., Kangas J., Mursula K., Molchanov O.A., Green J.A.* Pc 1–2 and Pc 4–5 pulsations observed at a network of high-latitude stations // J. Geophys. Res. – Space. V. 101. № 5. P. 10965–10973. 1996. https://doi.org/10.1029/95JA03770

24. *Prikner K., Mursula K., Kangas J., Kerttula, R., Feygin F.* An effect of the ionospheric Alfvén resonator on multiband Pc1 pulsations // Ann. Geophys. V. 22. № 2. P. 643–651. 2004. https://doi.org/10.5194/angeo-22-643-2004

25. *Safargaleev V., Kangas J., Kozlovsky A., Vasilyev A.* Burst of ULF noise excited by sudden changes of solar wind dynamic pressure // Ann. Geophys. V. 20. № 11. P. 1751–1761. 2002. https://doi.org/10.5194/angeo-20-1751-2002

26. *Safargaleev V., Kozlovsky A., Honary F., Voronin A., Turunen T.* Geomagnetic disturbances on ground associated with particle precipitation during SC // Ann. Geophys. V. 28. № 1. P. 247–265. 2010. https://doi.org/10.5194/angeo-28-247-2010

27. *Sucksdorff E.* Occurrences of rapid micropulsations at Sodankylä during 1932 to 1935 // Terrestrial Magnetism and Atmospheric Electricity. V. 41. № 4. P. 337–344. 1936. https://doi.org/10.1029/TE041i004p00337

28. *Tepley L.R., Wentworth R.C.* Hydromagnetic emission, X-rays, and electron bunches: 1. Experimental results // J. Geophys. Res. V. 67. № 9. P. 3317–3333. 1962. https://doi.org/10.1029/JZ067i009p03317

29. *Troitskaya V.A., Gul'elmi A.V.* Geomagnetic micropulsations and diagnostics of the magnetosphere // Space Sci. Rev. V. **7**. № 5–6. P. 689–768. 1967. https://doi.org/10.1007/BF00542894

30. *Young D. T., Perraut S., Roux A., de Villedary C., Gendrin R., Korth A., Kremser G., Jones D.* Wave-particle interactions near Ω_{He^+} observed on GEOS 1 and 2. 1. Propagation of ion cyclotron waves in He^+-rich plasma // J. Geophys. Res. – Space. V. 86. № 8. P. 6755–6772. 1981. https://doi.org/10.1029/JA086iA08p06755

FIGURE CAPTIONS

Fig. 1. Position of THE and GEOTAIL satellites before (upper panel) and after (lower panel) the sudden compression of the magnetosphere. The arrows show the direction of motion of the satellites.

Fig. 2. (*a*) Unstructured *Ps1* before and after SI (top two panels). Geomagnetic response to SI at high and low latitudes (bottom two panels). The arrows show the moments of the DMSP satellites flying over the observation region;

(*b*) pressure variations near the daily magnetopause on THE (upper panel) and variations of the interplanetary medium parameters on GEOTAIL (lower panel);
(*c*) variations of the interplanetary medium parameters at the WIND satellite.

Fig. 3. (*a*) Comparison of the unstructured *Pc1S* in LOZ with pressure variations at THE satellite (upper panel) and pulsations at HOR station (lower panel); (*b*) a series of unstructured spots in WAV (upper panel) and variations of the interplanetary medium parameters at GEOTAIL corrected for the propagation time from the satellite to the magnetopause (lower panel). Explanation in the text.

Fig. 4. Variations of the *Bz*- and By-component *of* the magnetic field on THE satellite as it leaves the magnetosphere for the transition region. $T_{MP}-$ moment of crossing the magnetopause. The magnetic barrier is marked in gray.

Fig. 5. (*a*) Pulsations on the IMAGE network up to the SI moment; (*b*) diagram illustrating the dynamics of equivalent ionospheric currents.

Fig. 6. (*a*) Spectrogram characterizing the rushes over the observation area showing the boundaries of the magnetospheric domains up to the SI moment; (*b*) position of the observation points relative to the magnetospheric boundaries (explanations in the text).

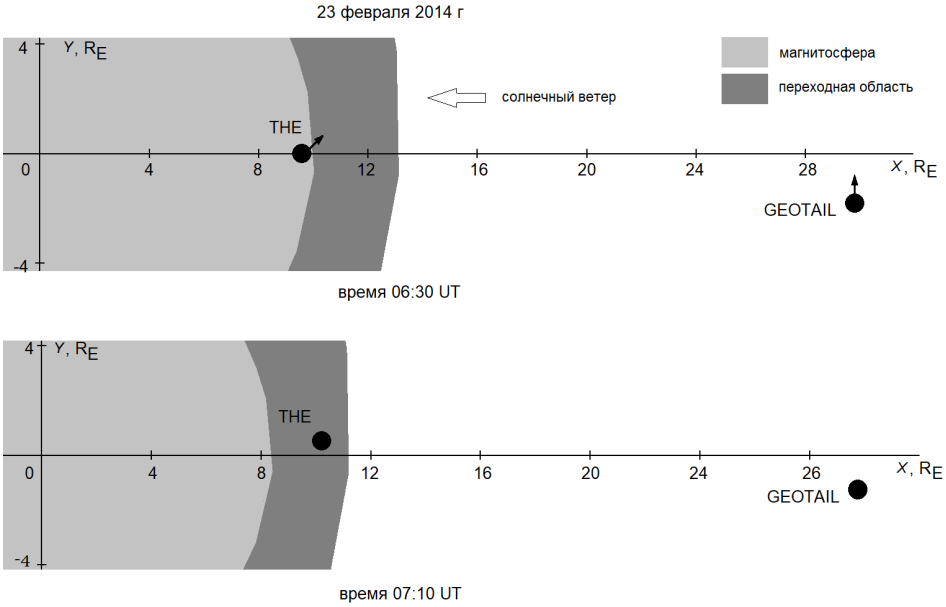
23 февраля 2014 г
4
Y, RE
0
4
8
12
16
20
24
28
X, RE
-4
THE
GEOTAIL
солнечный ветер
магнитосфера
переходная область
время 06:30 UT
4
Y, RE
0
4
8
12
16
20
24
26
X, RE
-4
THE
GEOTAIL
время 07:10 UT

Fig. 1.

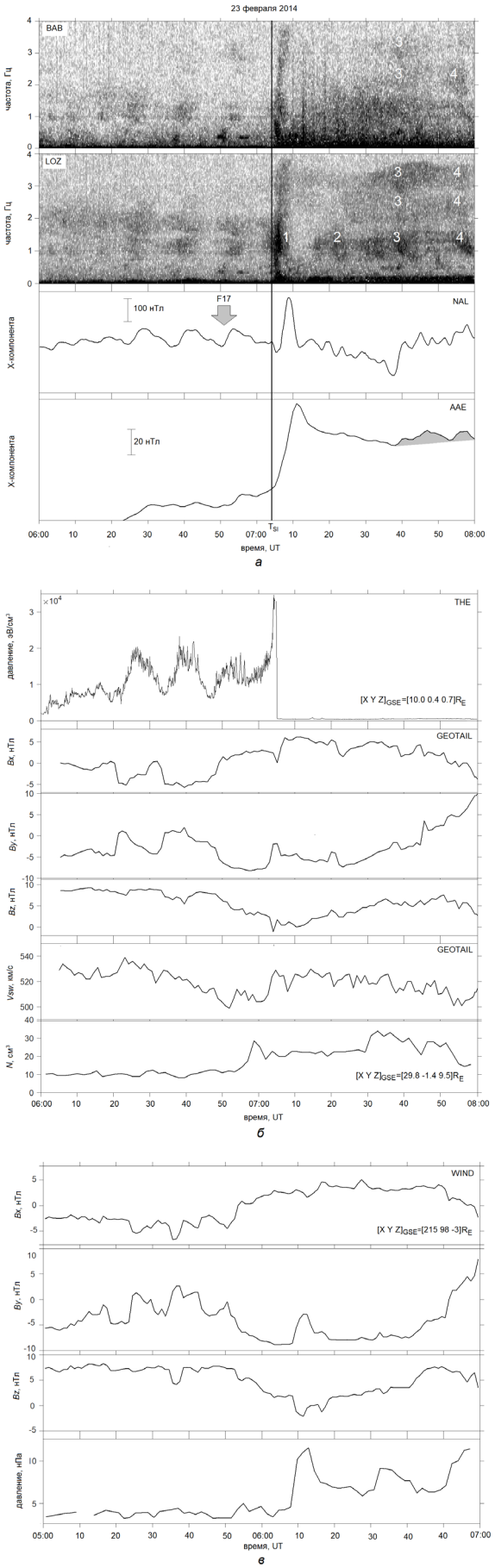
23 февраля 2014
BAB
LOZ
частота, Гц
1
2
3
4
100 нТл
F17
NAL
X-компонента
AAE
20 нТл
06:00
07:00
08:00
время, UT
а
THE
давление, эВ/см³
[X Y Z]GSE=[10.0 0.4 0.7]RE
GEOTAIL
Bx, нТл
By, нТл
Bz, нТл
Vsw, км/с
N, см³
[X Y Z]GSE=[29.8 -1.4 9.5]RE
б
WIND
[X Y Z]GSE=[215 98 -3]RE
давление, нПа
05:00
06:00
07:00
в

Fig. 2.

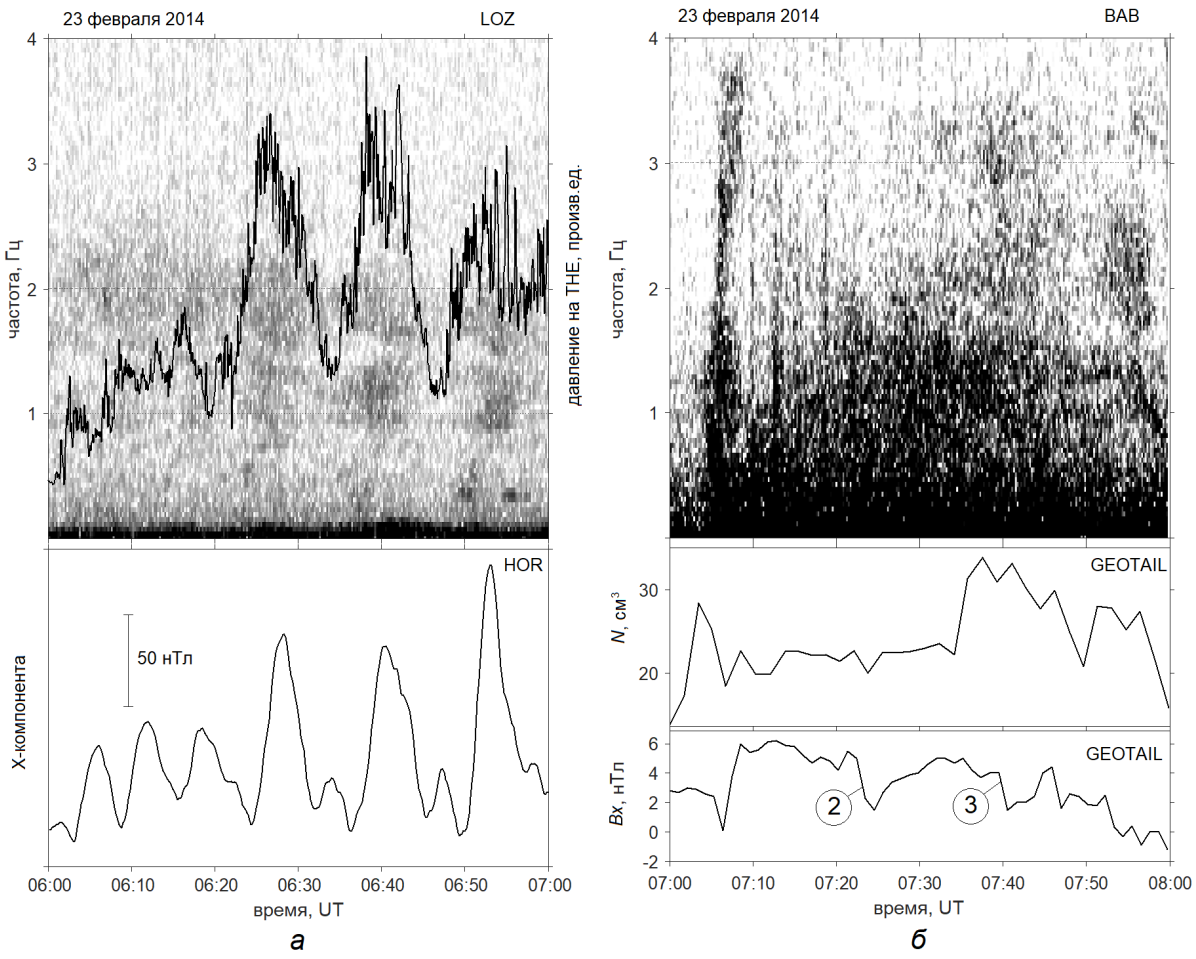
23 февраля 2014
LOZ
частота, Гц
давление на THE, произв.ед.
HOR
50 нТл
X-компонента
06:00
06:10
06:20
06:30
06:40
06:50
07:00
время, UT
а
23 февраля 2014
BAB
частота, Гц
GEOTAIL
N, см³
GEOTAIL
Bx, нТл
2
3
07:00
07:10
07:20
07:30
07:40
07:50
08:00
время, UT
б

Fig. 3.

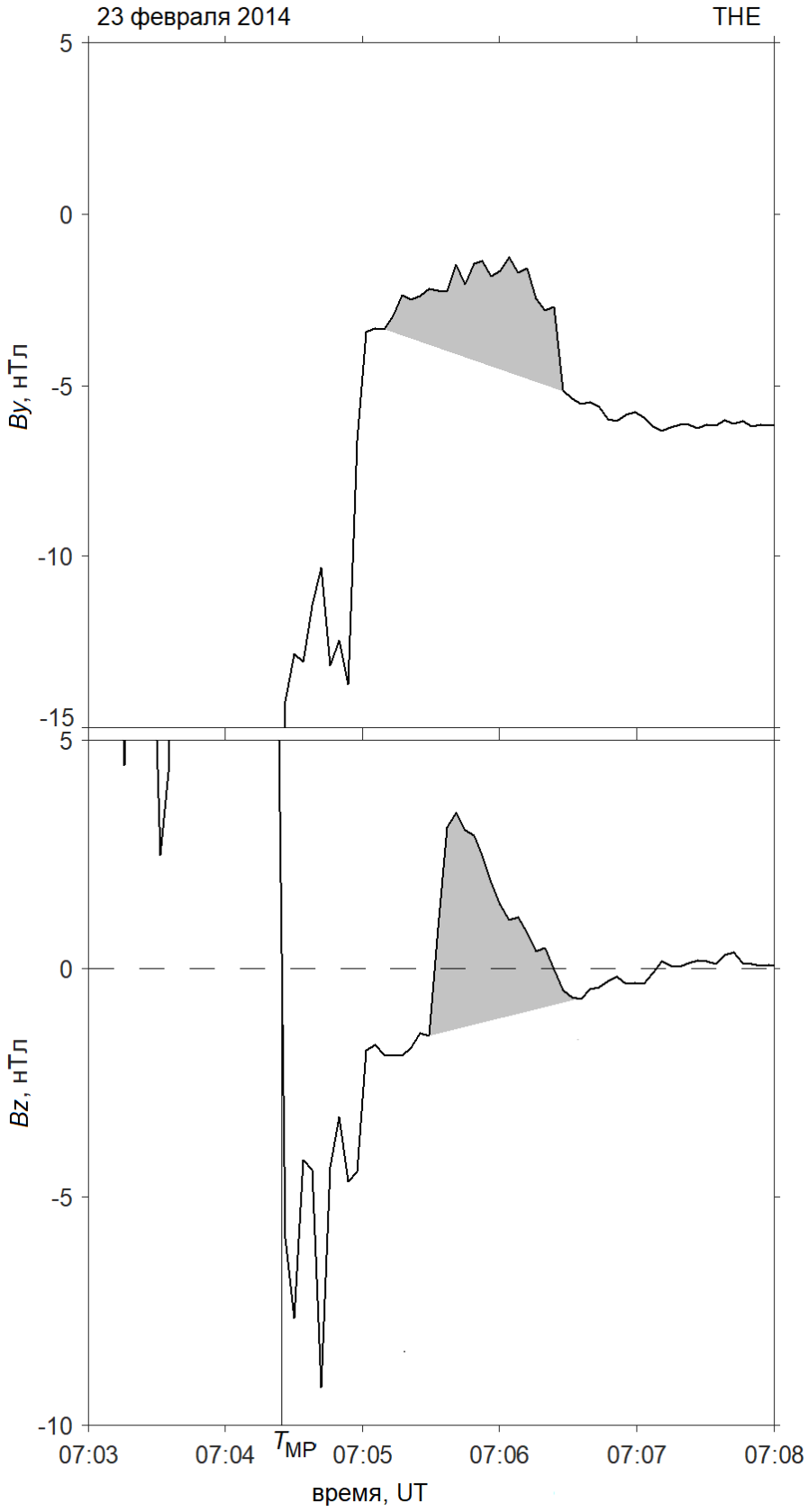
23 февраля 2014
THE
5
0
-5
-10
-15
By, нТл
5
0
-5
-10
Bz, нТл
07:03
07:04
T_{MP}
07:05
07:06
07:07
07:08
время, UT

Fig. 4.

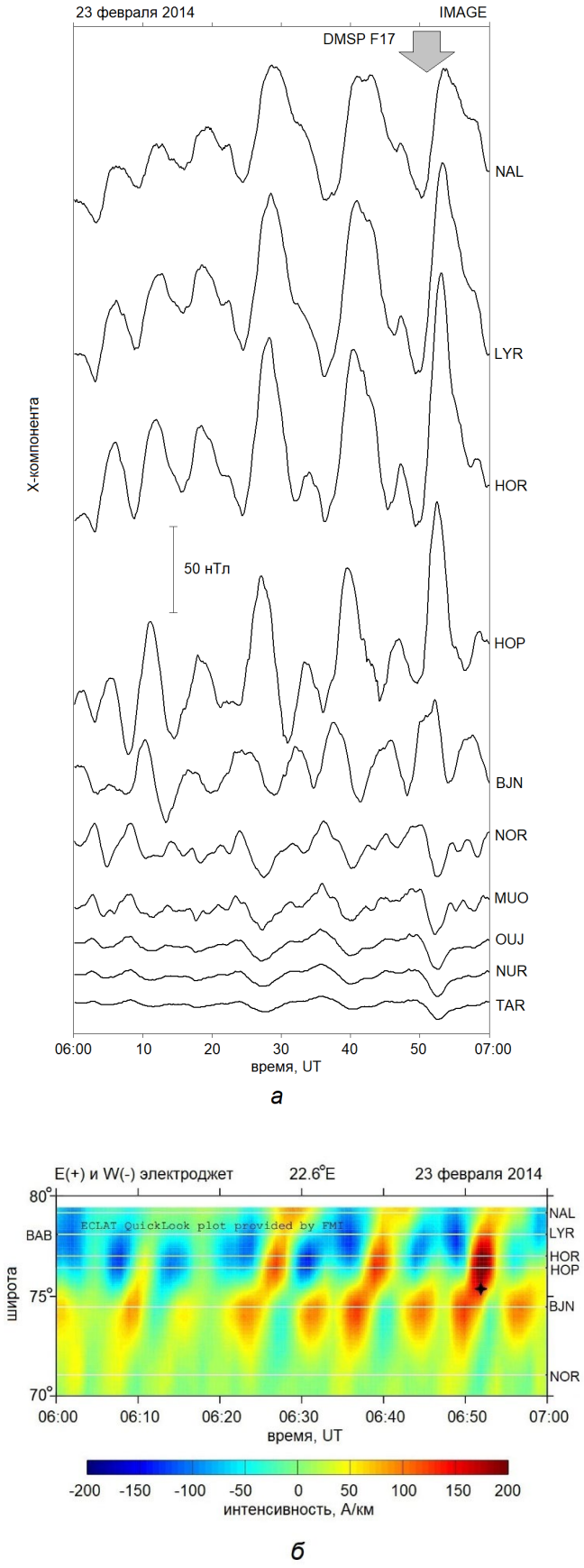
23 февраля 2014
IMAGE
DMSP F17
NAL
LYR
HOR
HOP
BJN
NOR
MUO
OUJ
NUR
TAR
50 нТл
X-компонента
06:00
10
20
30
40
50
07:00
время, UT
а
E(+) и W(-) электроджет
22.6°E
23 февраля 2014
80°
75°
70°
BAB
ECLAT QuickLook plot provided by FMI
NAL
LYR
HOR
HOP
BJN
NOR
широта
06:00
06:10
06:20
06:30
06:40
06:50
07:00
время, UT
-200
-150
-100
-50
0
50
100
150
200
интенсивность, А/км
б

Fig. 5.

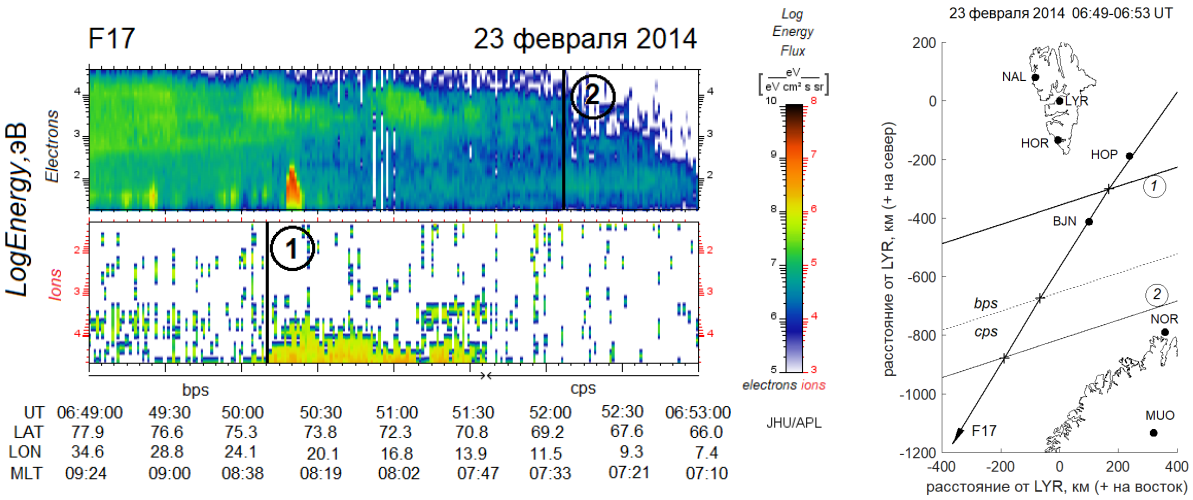
F17
23 февраля 2014
LogEnergy,эВ
Electrons
Ions
1
2
bps
cps
Log Energy Flux
[eV / eV cm² s sr]
electrons ions
JHU/APL
UT 06:49:00 49:30 50:00 50:30 51:00 51:30 52:00 52:30 06:53:00
LAT 77.9 76.6 75.3 73.8 72.3 70.8 69.2 67.6 66.0
LON 34.6 28.8 24.1 20.1 16.8 13.9 11.5 9.3 7.4
MLT 09:24 09:00 08:38 08:19 08:02 07:47 07:33 07:21 07:10
23 февраля 2014 06:49-06:53 UT
NAL
LYR
HOR
HOP
BJN
NOR
MUO
F17
bps
cps
расстояние от LYR, км (+ на север)
расстояние от LYR, км (+ на восток)

а *б*

Fig. 6.